Available online at www.sciencedirect.com

ScienceDirect

Journal of Nutritional Biochemistry 78 (2020) 108342

Journal of Nutritional Biochemistry

Impact of caloric restriction on AMPK and endoplasmic reticulum stress in peripheral tissues and circulating peripheral blood mononuclear cells from Zucker rats

Elena Vega-Martín[a], Raquel González-Blázquez[b], Francisco J. Manzano-Lista[a], Miriam Martín-Ramos[b], Concepción F. García-Prieto[b], Marta Viana[c], Miguel A. Rubio[d], Alfonso L. Calle-Pascual[d,e], Lillà Lionetti[f], Beatriz Somoza[b], María S. Fernández-Alfonso[a], Martín Alcalá[c,1], Marta Gil-Ortega[b,*,1]

[a]*Instituto Pluridisciplinar, Facultad de Farmacia, Universidad Complutense de Madrid, 28040 Madrid, Spain*
[b]*Departamento de Ciencias Farmacéuticas y de la Salud, Facultad de Farmacia, Universidad San Pablo-CEU, CEU Universities, 28925, Madrid, Spain*
[c]*Departamento de Química y Bioquímica, Facultad de Farmacia, Universidad San Pablo-CEU, CEU Universities, 28925, Madrid, Spain*
[d]*Department of Endocrinology and Nutrition, Hospital Clínico San Carlos, Instituto de Investigación Sanitaria San Carlos (IdISSC), Facultad de Medicina, Complutense University, C/ Prof. Martin Lagos s/n, 28040 Madrid, Spain*
[e]*Centro de Investigación Biomédica en Red de Diabetes y Enfermedades Metabólicas Asociadas (CIBERDEM), Madrid, Spain*
[f]*Department of Chemistry and Biology "A. Zambelli", University of Salerno, Via Giovanni Paolo II, 132, Fisciano, 84084, Italy*

Received 11 June 2019; received in revised form 27 December 2019; accepted 3 January 2020

Abstract

The activation of endoplasmic reticulum (ER) stress and a reduction of AMP-dependent protein kinase (AMPK) phosphorylation have been described in obesity. We hypothesize that a moderate caloric restriction (CR) might contribute to reducing ER stress and increasing AMPK phosphorylation in peripheral tissues from genetically obese Zucker *fa/fa* rats and in peripheral blood mononuclear cells (PBMCs).

Zucker *Lean* and Zucker *fa/fa* rats were fed with chow diet either *ad libitum* (AL) (C, as controls) or 80% of AL (CR) for 2 weeks, giving rise to four experimental groups: *Lean* C, *Lean* CR, *fa/fa* C and *fa/fa* CR.

CR significantly increased AMPK phosphorylation in the liver, perirenal adipose tissue (PRAT) and PBMCs from *fa/fa* rats but not in the subcutaneous AT (SCAT), suggesting a reduced response of SCAT to CR. Liver samples of *fa/fa* rats exhibited an increased mRNA expression of PERK, EIF-2α, XBP-1(s), Chop and caspase 3, which was significantly reduced by CR. PRAT exhibited an overexpression of Edem and PDIA-4 in *fa/fa* rats, but only PDIA-4 expression was reduced by CR. eIF-2α phosphorylation was significantly increased in all studied tissues from *fa/fa* rats and reduced by CR. A negative correlation was detected between p-AMPK and p-eIF-2α in the liver, PRAT and PBMCs from *fa/fa* rats but not in SCAT.

This study shows that a moderate CR reduces ER stress and improves AMPK phosphorylation in several peripheral tissues and in circulating PBMCs, suggesting that alterations observed in PBMCs could reflect metabolic alterations associated with obesity.

Keywords: Caloric restriction; Endoplasmic reticulum stress; Obesity; AMPK; Circulating peripheral blood mononuclear cells

1. Introduction

Obesity is nowadays one of the most worrying epidemic health problems in our society. One of the most remarkable changes that take place during the onset of obesity is the expansion of adipose tissue (AT) due to an increase in adipocyte size (hypertrophy) and number (hyperplasia). However, the expansibility of AT is limited [1], and an excessive expansion of AT has been related with numerous diseases, including insulin resistance, type 2 diabetes, cardiovascular disease and cancer [2].

The endoplasmic reticulum (ER) is a multifunctional organelle essential for the synthesis, folding and processing of secretory and transmembrane proteins. For a proper protein folding, a balance between ER protein load and the folding capacity to process this load must be established. However, physiological and pathological stimuli can disrupt ER homeostasis, resulting in an accumulation of misfolded and unfolded proteins, a condition known as ER stress. ER stress activates a complex signaling network referred as the unfolded protein response (UPR) to reduce stress and restore homeostasis. However, if UPR fails to reduce ER stress, it causes cell dysfunction and death. Chronic activation of the UPR

* Corresponding author at: Universidad CEU San Pablo, Facultad de Farmacia, Ctra. Boadilla del Monte Km 5.300, 28925, Alcorcón, Madrid, (Spain). Tel.: +34 913724700; fax: +34 913724775.
E-mail address: mgortega@ceu.es (M. Gil-Ortega).
[1] These authors contributed equally.

https://doi.org/10.1016/j.jnutbio.2020.108342
0955-2863/

has been described in both dietary and genetic models of obesity [3]. In addition, several studies have evidenced a role of ER stress in the development of cardiometabolic disorders [4–6], insulin resistance (reviewed in Lionetti et al., 2009 [7]) and hepatic steatosis (reviewed in Mollica et al., 2011 [8]). GRP78, also known as BiP, is a master regulator for ER stress and responsible for the activation of UPR signaling [9]. One of the proteins implicated in initiating UPR signaling is the double-stranded RNA-dependent protein kinase-like ER kinase (PERK), whose activation leads to the phosphorylation of the α-subunit of the translation initiation factor eIF2 (p-eIF-2α), one of the most widely used markers of ER stress [10,11]. IRE-1 constitutes the master regulator of the reparative branch of the UPR. IRE-1 activation leads to X-box binding protein 1 (XBP-1) splicing and accounts for an up-regulation of UPR target genes, including the ER-degradation-enhancing-α-mannidose-like protein (Edem) or the protein disulfide-isomerase A4 (Pdia-4) [12–15]. In addition, it is known that, under acute ER stress, the expression of apoptotic markers like CHOP is markedly stimulated through IRE1- and PERK-mediated signaling [16].

AMP-dependent protein kinase (AMPK) is considered as a key metabolic sensor that contributes to restore energy homeostasis [17]. The reduction of AMPK activation (through its phosphorylation at Thr^{172}) during the development of obesity [18,19] contributes to the pathogenesis of insulin resistance and metabolic-syndrome-associated diseases [18]. To the contrary, activation of AMPK by caloric restriction (CR) has been shown to exert beneficial effects on several alterations associated with obesity like insulin resistance, dyslipidemias [20,21], hypertension or endothelial dysfunction [22].

Several studies have suggested a link between ER stress and AMPK activity. Indeed, whereas AMPK inhibition is associated with an increased ER stress [23], AMPK activation reduces ER stress in several tissues like the kidney or the vasculature [24,25]. A 50% CR in genetically obese mice (*ob*/*ob*) accounted for a significant reduction of ER stress as shown by the reduction of eIF-2α phosphorylation levels [26]. However, those studies have been performed in different models subjected to a very severe CR (greater than 40%).

Several studies performed in peripheral mononuclear blood cells (PBMCs) have revealed a link between their mitochondrial physiology and both the nutritional status and several metabolic alterations [27,28]. A recent study from our group shows a significant reduction of p-AMPK levels in PMBCs cells from obese patients which was reversed by bariatric surgery [20]. This is a relevant finding since PBMCs are easily obtained from peripheral blood samples and may emerge as potential interesting cells for the screening of several metabolic changes observed in peripheral tissues.

In this context, we hypothesize that a short-term moderate (20%) CR in a genetic model of obesity (the Zucker *fa*/*fa* rat) (1) activates AMPK and reduces ER stress in liver and adipose tissues and (2) that these changes are detected in PBMCs as markers of metabolic status. With this goal, we assessed (1) body weight, liver weight and the amount of both visceral (perirenal, PRAT) and subcutaneous adipose tissue (SCAT); (2) lipid content in liver and adipocytes' diameter in fat depots; (3) p-AMPK/AMPK and p-eIF-2α/eIF-2α in the liver, PRAT and SCAT; (4) mRNA expression of ER stress [BiP, eIF-2α, XBP-1(s), EDEM and Pdia-4] and apoptosis (CHOP and caspase 3) markers and (5) a potential association between p-eIF-2α and p-AMPK in those tissues. Moreover, we aimed at elucidating whether p-eIF-2α and p-AMPK levels in PBMCs could mirror the metabolic changes observed in the liver and fat depots.

2. Materials and methods

2.1. Animals and dietary treatments

Eight-week-old male Zucker *Lean* and Zucker *fa*/*fa* rats were housed under controlled dark–light cycles (12 h/12 h from 8:00 a.m. to 8:00 p.m.) and temperature (22°C) conditions with standard food and water *ad libitum* (AL). Animals (n=8 per group) were housed individually for body weight (BW) and food intake monitoring for 4 weeks, divided into two groups with a similar mean BW and assigned either to an *ad libitum* (C) or a calorie-restricted diet (CR; 80% of AL) for 2 additional weeks. Twenty percent caloric restriction was calculated individually based on previous food intake values. On the last day, rats were weighed and anesthetized (80 mg/kg ketamine hydrochloride and 8 mg/kg xylazine i.p.), blood was collected by cardiac puncture, and rats were subsequently euthanized by decapitation. Adipose tissues and liver were weighed and frozen at −80°C for their subsequent use. The investigation was performed in accordance with the recommendations of the Spanish Animal Care and Use Committee according to the EC Directive 86/609/EEC for animal experiments and was approved by both the Ethical Committee of Universidad San Pablo-CEU (CEBA-CEU USP, reference: PCD 050-1V3/12) and Universidad Complutense de Madrid, Spain (reference: PROEX413/15). All efforts were made to avoid animal suffering, and studies involving animals are reported in accordance with the ARRIVE guidelines for reporting experiments involving animals [29,30].

2.2. Measurement of total lipid content in liver

Lipids were extracted from liver in chloroform/methanol (2/1) following the method of Folch with modifications [31].

2.3. Measurement of adipocyte diameter in PRAT and SCAT

Intact PRAT and SCAT samples were fixed in 4% PFA, cut in 1–2-mm^3 pieces, placed on a slide and visualized with the help of a confocal microscope (Leica Microsystems, Wetzlar, Germany). Adipocyte diameter was measured with an image analysis program (Image J, Boston, MA, USA).

2.4. Blood collection

Blood samples from anesthetized nonfasted Zucker rats were collected in heparinized tubes and submitted to two different procedures: (1) blood samples were centrifuged at 3000 rpm for 10 min at 4°C to obtain plasma, and (2) blood samples were diluted with PBS (pH=7.4) (1:1 ratio) and submitted to Ficoll–Hypaque (Sigma-Aldrich) density gradient. After centrifugation at 1800 rpm for 30 min at 4°C, the mononuclear cells interface was collected, washed with PBS and centrifuged at 1200/1500 rpm for 5 min at 4°C. Then, the pellet containing PBMCs was collected. Both plasma and PBMCs samples were frozen at −80°C.

2.5. Protein isolation from liver, PRAT, SCAT and PBMCs

Liver and PBMCs were homogenized in a lysis buffer containing (0.42 mM NaCl, 1 mM $Na_4P_2O_7$, 1 mM dichloro diphenyl trichloroethane, 20 mM HEPES, 20 mM NaF, 1 mM Na_3VO_4, 1 mM EDTA, 1 mM EGTA, 20% glycerol, 2 mM phenylmethylsulfonyl fluoride (PMSF), 1 μl/ml leupeptin, 1 μl/ml aprotinin and 0.5 μl/ml N-α-p-tosyl-1-lysine in chloromethylketone (TLCK) with a Tissue Lyser homogenizer (Qiagen, Hilden, Germany) applying one cycle of 2 min at 50 Hz or a manual potter, respectively. Samples were subjected to three thermal shocks (37°C water bath/liquid nitrogen) and centrifuged for 10 min at 10,000*g* at 4°C, and supernatants were collected.

PRAT and SCAT were homogenized in a lysis buffer containing 1 mM $Na_4P_2O_7$, 20 mM HEPES, 20 mM NaF, 1 mM Na_3VO_4, 1 mM EDTA, 0.1% Triton X-100, 20% glycerol, 1 μl/ml leupeptin, 1 μl/ml aprotinin and 0.5 μl/ml TLCK with a Tissue Lyser homogenizer (Qiagen) by applying two cycles of 2 min at 50 Hz. Samples were left on ice for 20 min, shaken every 5 min and centrifuged for 30 min at 17,000*g* at 4°C,

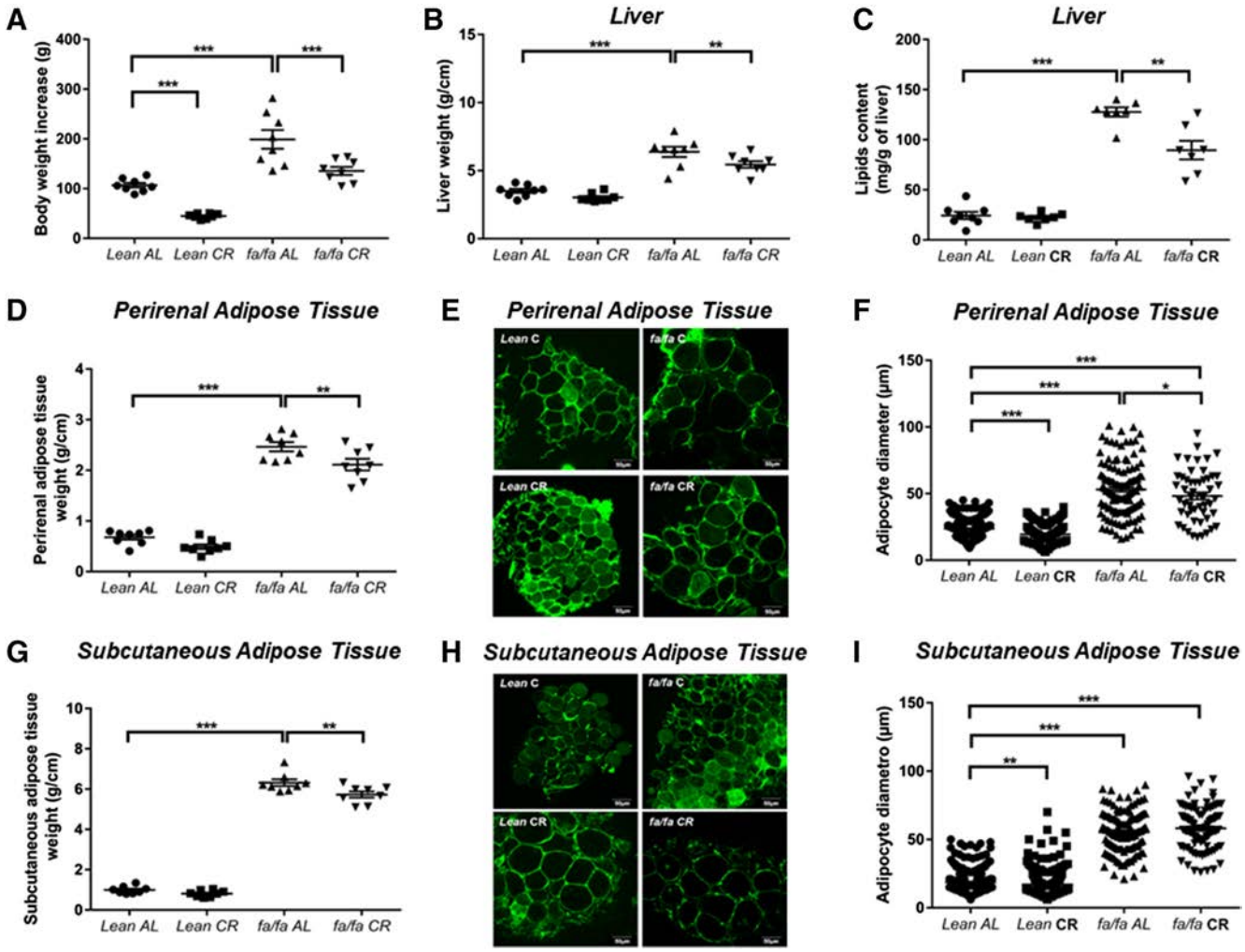

Fig. 1. Dot-blot graphs show animals' body weight increase (A); the weight of the liver (B), PRAT (D) and SCAT (G); and the lipid content in the liver (C). Representative confocal projections of PRAT (E) and SCAT (H) samples. Dot-blot graphs show quantification of adipocytes' diameter from PRAT (F) and SCAT (I). Each result represents the mean±S.E.M. (n=8). $^{**}P$<.01 and $^{***}P$<.001, compared to *Lean* C group; $^{\#}P$<.05, $^{\#\#}P$<.01 and $^{\#\#\#}P$<.001, compared to *fa*/*fa* C group (one-way ANOVA; Newman–Keuls *post hoc* test).

and supernatants were collected. Protein concentration was determined using the method described by Bradford [32].

2.6. Western blot analysis

Western blot studies were performed on liver, PRAT, SCAT and PBMCs samples as previously described [33]. Briefly, 30-µg protein samples were separated by SDS-PAGE gels. Primary antibodies against p-AMPKα (Thr172), AMPKα (1: 1000 final dilution; Cell Signaling Technology, Danvers, MA, USA), p-eIF-2α(Ser^{51}) and eIF-2α (1: 500 final dilution; Cell Signaling Technology) were applied overnight at 4 °C. After washing, appropriate secondary antibodies (anti-rabbit or anti-mouse IgG-peroxidase conjugated) were applied for 1 h at a dilution of 1:5000. Blots were washed and incubated in commercial enhanced chemiluminescence reagents (ECL Prime, GE Healthcare, Little Chalfont, UK), and bands were detected by ChemiDoc XRS+ Imaging System (BioRad, Alcobendas, Spain). To prove equal loadings of samples, blots were incubated with β-actin antibody (1:5000 final dilution; Sigma-Aldrich). Blots were quantified using Image Lab 3.0 software (BioRad). Values for pAMPKα (Thr^{172}) and pEIF-2α (Ser^{51}) were normalized with AMPK and eIF-2α, respectively.

2.7. RNA extraction and real-time PCR (RT-qPCR)

Total RNA was isolated from the liver, PRAT and SCAT using Qiazol Reagent (Qiagen). The samples were processed using an RNeasy Mini Kit (Qiagen), and the concentration and purity of RNA were assessed with NanoVue (GE Healthcare). Reverse transcription was performed on 500 ng of RNA with iScript cDNA synthesis kit (BioRad) using random hexamer primers. Optimal annealing temperature and amplicon sizes were checked for each pair of primers. RT-qPCR analyses were performed in a CFX96 Instrument (BioRad). A total of 6.25 ng of cDNA from four samples of each group were run in duplicate, and the mRNA levels were determined using intron-skipping primers, TBP as a housekeeping gene and SYBR Green Master Mix (Applied Biosystems, Foster City, CA, USA). All primer sequences are detailed in Supplementary Information 1.

2.8. Data analyses

All values are given as mean±S.E.M., and n denotes the number of animals used in each experiment. Statistical significance was analyzed using one-way analysis of variance (ANOVA) followed by Newman–Keuls *post hoc* test for comparison between groups. Correlation

analysis was performed through linear regression as well as analyzed by Pearson's correlation. A value of $P<.05$ was considered statistically significant. Statistical analysis was performed with GraphPad Prism 7.0 (GraphPad Software, La Jolla, CA, USA).

3. Results

3.1. Caloric restriction decreased body, liver and adipose tissue weight in fa/fa Zucker rats

As shown in Fig. 1A, at the end of the protocol, BW increase was significantly higher in *fa/fa* rats than in *Lean* rats ($P<.001$). CR significantly reduced BW in both *fa/fa* and *Lean* rats when compared to their respective AL-fed controls ($P<.001$, Fig. 1A). The weight of the liver, PRAT and SCAT was significantly higher in *fa/fa* animals than in *Lean* animals but reduced by CR (Fig. 1B, D and E).

3.2. Caloric restriction decreased total lipid content in liver and adipocyte size in PRAT from fa/fa Zucker rats

Total lipid content was higher in the liver from *fa/fa* C rats compared to the *Lean* C group ($P<.001$). CR significantly reduced total lipid content only in *fa/fa* animals ($P<.01$), but no changes were detected in the *Lean* group (Fig. 1C).

Adipocyte diameter was significantly higher in PRAT (Fig. 1E and F) and SCAT (Fig. 1H and I) from *fa/fa* C rats than in the *Lean* C group ($P<.001$). CR significantly decreased adipocyte size ($P<.01$) in PRAT. However, CR did not reduce adipocyte diameter in SCAT, evidencing a higher sensitivity of visceral AT to short-term CR.

3.3. Caloric restriction increases AMPK phosphorylation in liver, PRAT and PBMCs from fa/fa Zucker rats

Levels of p-AMPK$^{Thr\text{-}172}$/AMPK were significantly lower in the liver, PRAT, SCAT and PBMCs from *fa/fa* C animals compared to the *Lean* C group (Fig. 2A–D; $P<.05$). CR significantly enhanced AMPK phosphorylation in the liver, PRAT and PBMCs from *fa/fa* animals (Fig. 2A, B and D; $P<.05$) but remained unmodified in SCAT (Fig. 2C). These results again suggest a reduced sensitivity of SCAT to CR compared to PRAT, the liver or PBMCs.

3.4. Caloric restriction ameliorates obesity-induced UPR response in liver from fa/fa Zucker rats

To analyze the effect of obesity and CR in ER stress in the liver, PRAT and SCAT, we measured the expression of key mediators in the different UPR branches.

In the liver, the expression of the general activator BiP (Fig. 3A) exhibited a five-fold increase in mRNA levels compared to the *Lean* C group. This was significantly reduced after mild CR. A nonsignificant trend to increased mRNA levels was observed in the *Lean* CR group compared to the *Lean* C rats.

A similar pattern was observed in the members of the PERK-mediated branch of the UPR. mRNA levels of eIF-2α were significantly higher in the *fa/fa* group compared to their *lean* counterparts (Fig. 3B).

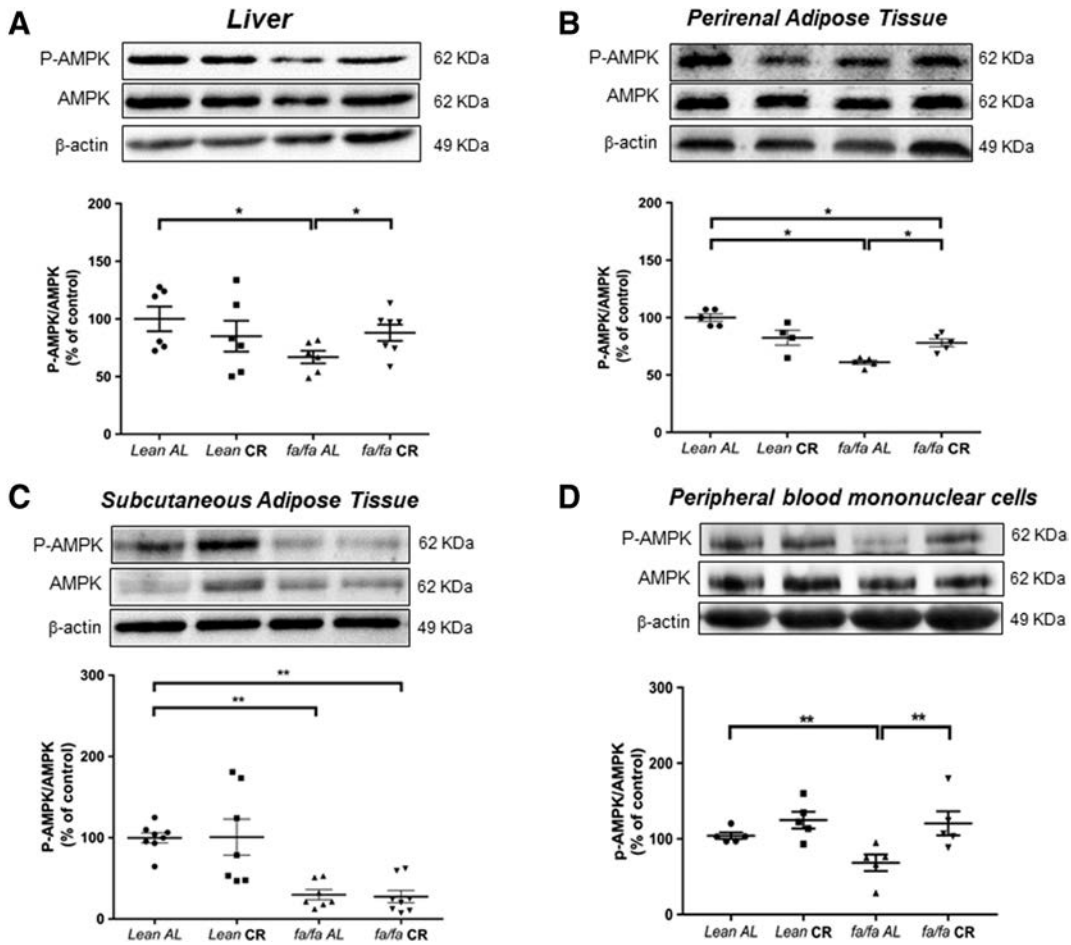

Fig. 2. Representative immunoblots of p-AMPK/AMPK and β-actin expression in the liver (A; $n=6$–7), PRAT (B; $n=5$), SCAT (C; $n=7$–8) and peripheral mononuclear blood cells (D; $n=5$) from *Lean* and *fa/fa* rats submitted or not to caloric restriction. Dot-blot graphs show the result of densitometric analysis of p-AMPK/AMPK immunoblots expressed as percentage of p-AMPK/AMPK in the *Lean* C group. $^{*}P<.05$ and $^{**}P<.01$, compared to *Lean* C group; $^{\#}P<.05$ and $^{\#\#}P<.01$, compared to *fa/fa* C group (one-way ANOVA; Newman–Keuls *post hoc* test).

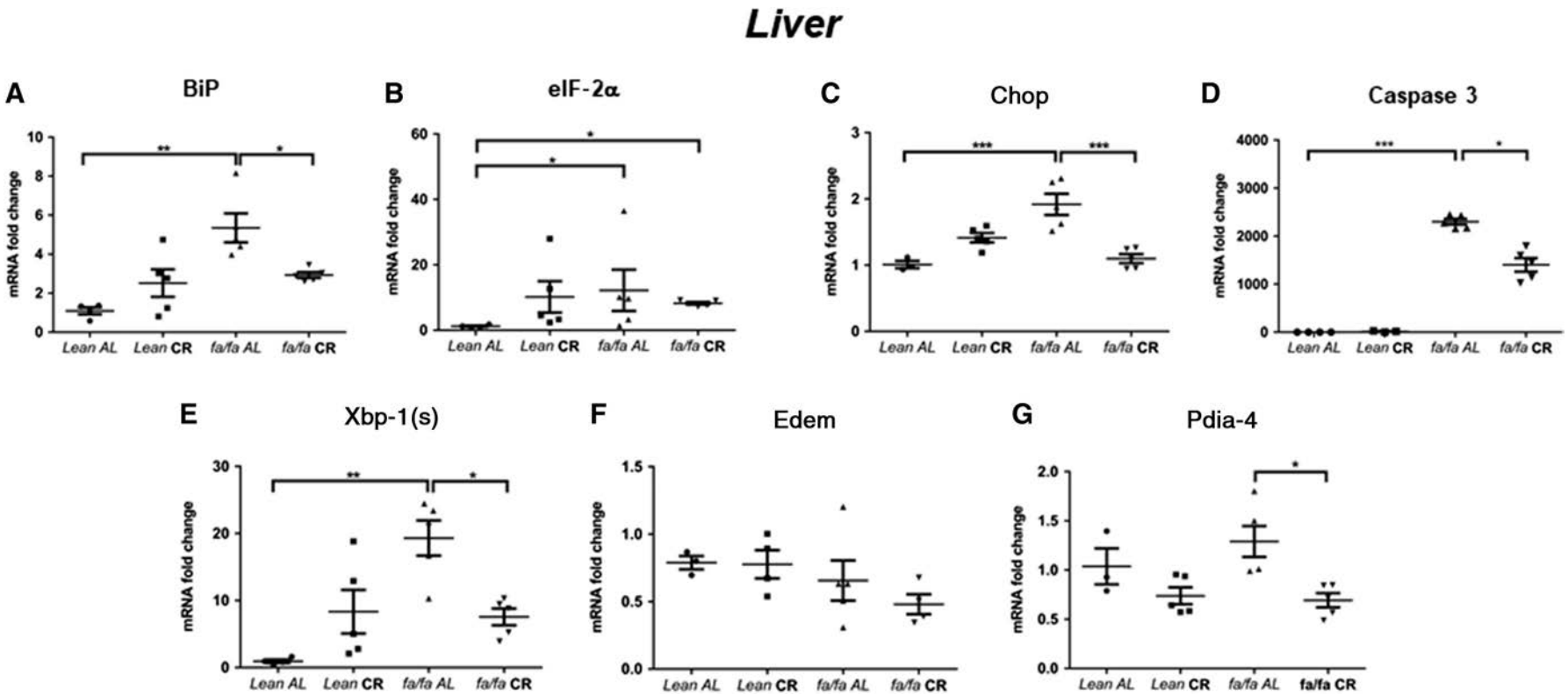

Fig. 3. Dot-blot graphs show mRNA expression of BiP (A), eIF-2α (B), Chop (C), Caspase 3 (D), Xbp-1(s) (E), Edem (F) and Pdia-4 (G) in samples of liver from *Lean* and *fa/fa* rats submitted or not to caloric restriction. Each result represents the mean±S.E.M. (n=4–5). $^{*}P$<.05, $^{**}P$<.01 and $^{***}P$<.001, compared to *Lean* C group; $^{\#}P$<.05 and $^{\#\#\#}P$<.001, compared to *fa/fa* C group (one-way ANOVA; Newman–Keuls *post hoc* test).

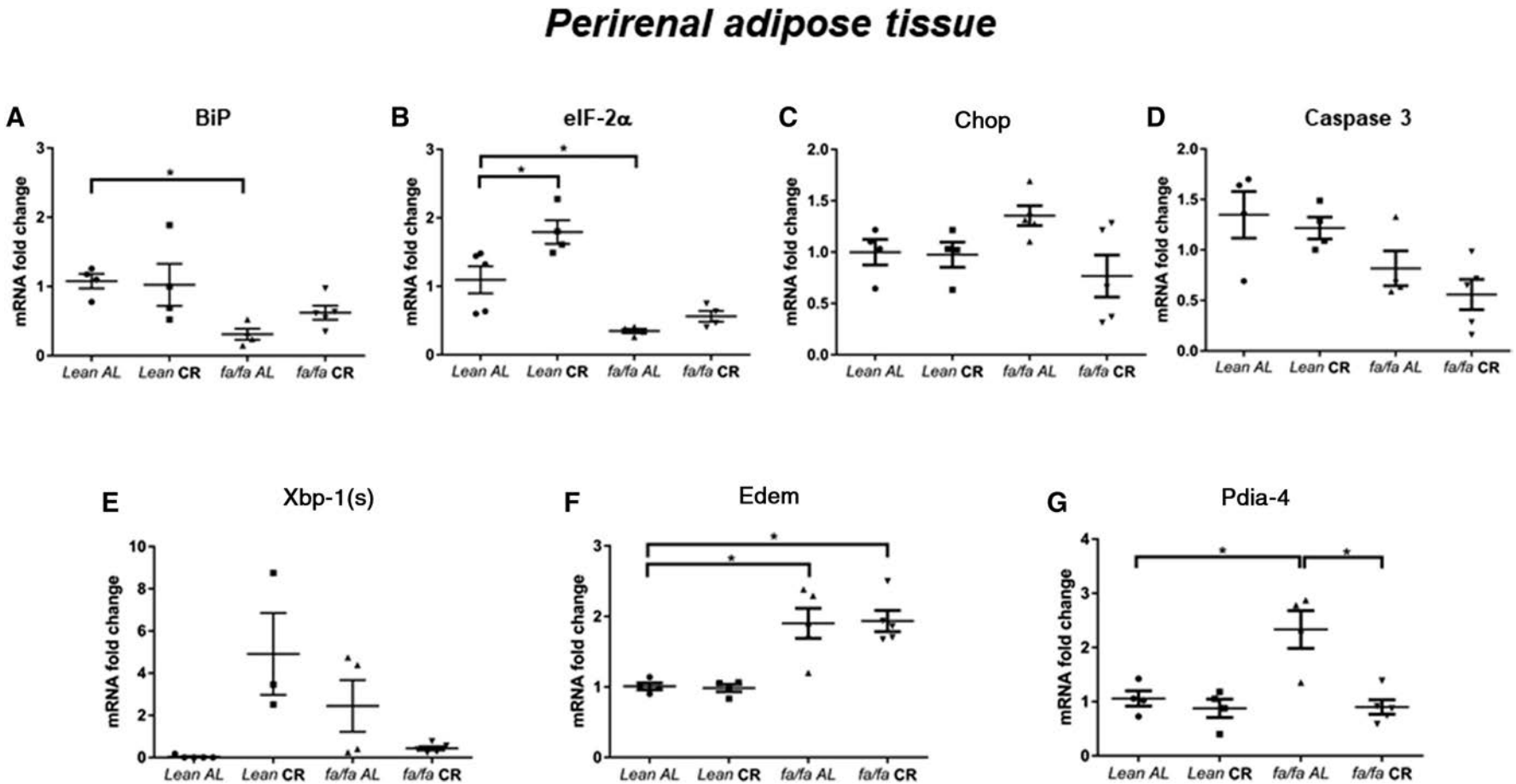

Fig. 4. Dot-blot graphs show mRNA expression of BiP (A), eIF-2α (B), Chop (C), Caspase 3 (D), Xbp-1(s) (E), Edem (F) and Pdia-4 (G) in samples of PRAT from *Lean* and *fa/fa* rats submitted or not to caloric restriction. Each result represents the mean±S.E.M. (n=4–5). $^{*}P$<.05, compared to *Lean* C group; $^{\#}P$<.05, compared to *fa/fa* C group (one-way ANOVA; Newman–Keuls *post hoc* test).

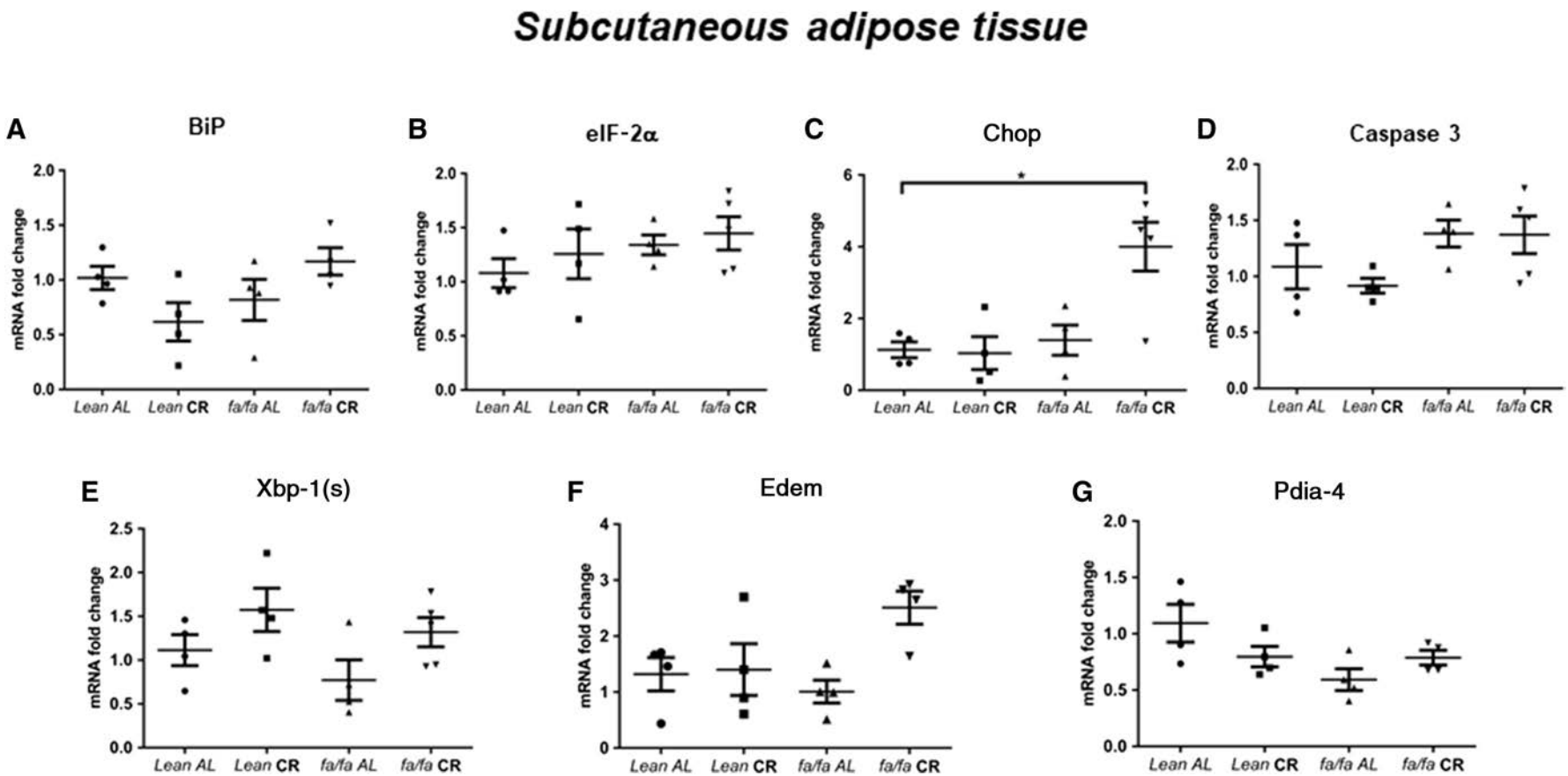

Fig. 5. Dot-blot graphs show mRNA expression of BiP (A), eIF-2α (B), Chop (C), Caspase 3 (D), Xbp-1(s) (E), Edem (F) and Pdia-4 (G) in samples of SCAT from *Lean* and *fa/fa* rats submitted or not to caloric restriction. Each result represents the mean±S.E.M. (n=4–5). *P<.05, compared to *Lean* C group (one-way ANOVA; Newman–Keuls *post hoc* test).

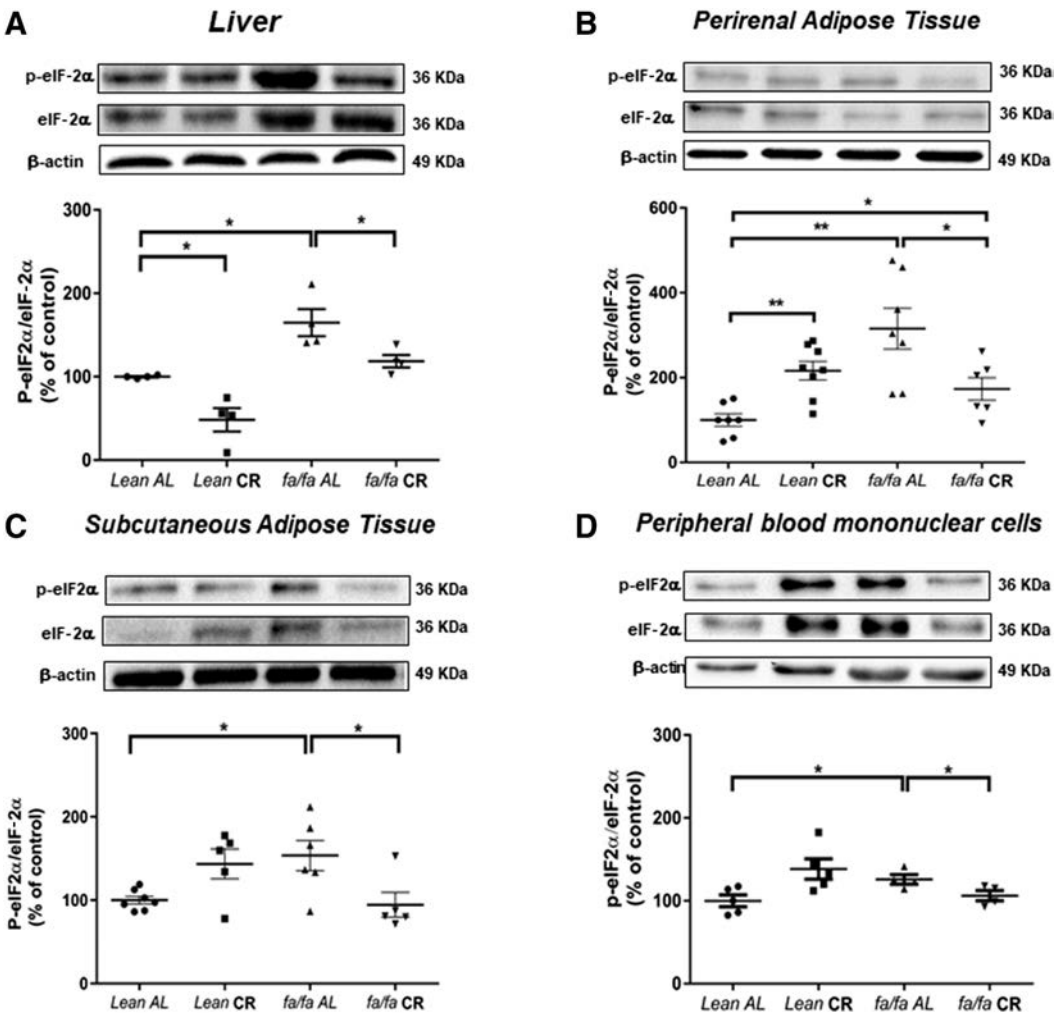

Fig. 6. Representative immunoblots of p-eIF-2α/eIF-2α and β-actin expression in the liver (A; $n=4$), PRAT (B; $n=6$–8), SCAT (C; $n=5$–7) and PBMCs (D; $n=5$) from *Lean* and *fa/fa* rats submitted or not to caloric restriction. Dot-blot graphs show the result of densitometric analysis of p-eIF-2α/eIF-2α immunoblots expressed as percentage of p-eIF-2α/eIF-2α in the *Lean* C group. $^{*}P<.05$ and $^{**}P<.01$, compared to *Lean* C group; $^{\#}P<.05$ compared to *fa/fa* C group (one-way ANOVA; Newman–Keuls *post hoc* test).

CR reduced eIF-2α mRNA levels in *fa/fa* animals and caused a nonsignificant increase in the *Lean* C.

Regarding the proapoptotic markers Chop and Caspase 3, *fa/fa* C rats showed a significant spike in the mRNA levels of both markers, with an effective role of CR to moderate their expression. No CR change was observed in *Lean* animals (Fig. 3C and D). However, the analyses of the intrinsic apoptotic pathway through the quantification of the mRNA levels of the proapoptotic Bax gene and the antiapoptotic Bcl2 gene revealed no changes in the Bax/Bcl2 ratio in the liver of *fa/fa* rats. Nonetheless, CR accounted for a 50% reduction in this ratio (Supplementary Fig. 1).

In relation to the reparative branch of the UPR triggered by IRE-1, the mediator Xbp-1(s) showed a significant 20-fold increase in *fa/fa* C rats when compared to *Lean* C, which was effectively reduced by the moderate CR (Fig. 3E). A nonsignificant increase was observed in *Lean* CR rats. However, these changes in the Xbp-1(s) expression are not translated into changes in the expression of the downstream chaperones Edem and Pdia4 (Fig. 3F and G). No changes were observed among any of the four groups in the mRNA levels of Edem, while only a reduction in Pdia-4 expression was observed in the *fa/fa* CR when compared to *fa/fa* C.

3.5. Caloric restriction reduces gene expression of ER stress and apoptotic markers in PRAT and SCAT from fa/fa Zucker rats

The analysis of the UPR pathway in the adipose tissue revealed a depot-dependent effect. In the PRAT, we did not find any difference in the expression of BiP among any of the four experimental groups (Fig. 4A). eIF-2α mRNA levels were up-regulated in the *Lean* CR group and reduced in the *fa/fa* C when compared to the *Lean* C (Fig. 4B). Finally, no differences were observed in the apoptotic mediators Chop and Caspase 3 (Fig. 4C and D). However, we found differences in the reparative branch of the UPR. While no statistical significance was achieved in the expression of Xbp-1(s) among any of the four groups (Fig. 4E), the *fa/fa* C group exhibited a two-fold increase in the expression of the chaperones Edem and Pdia-4. CR was only able to return to *Lean* C mRNA expression levels in the case of Pdia-4 (Fig. 4F and G).

In the SCAT, the effect of the genetic obesity and the CR was not enough to trigger the UPR response. No significant differences were observed in the expression of any of the studied mediators among any of the four groups (Fig. 5), except for an up-regulation in Chop in the *fa/fa* CR vs. the *Lean* C (Fig. 5C).

3.6. Caloric restriction reduces p-eIF-2α/eIF-2α in liver, PRAT, SCAT and PBMCs from fa/fa Zucker rats

The ratio p-eIF-2α / eIF-2α was significantly higher in the liver, PRAT, SCAT and PBMCs from *fa/fa* C animals compared to the *Lean* C group ($P<.05$, Fig. 6) but significantly reduced by CR in all tissues from *fa/fa* animals ($P<.05$; Fig. 6). p-eIF-2α/eIF-2α ratio was higher in PRAT and SCAT from the *Lean C* group ($P<.01$ and $P<.05$; Fig. 6) compared to

the *Lean* CR group. CR did not modify p-eIF-2α/eIF-2α levels in PBMCs from *Lean* rats (Fig. 6B).

3.7. Levels of p-eIF-2α negatively correlate with p-AMPK levels in liver, PRAT and PBMCs

A negative correlation was detected between the degree of phosphorylation of AMPK and eIF-2α in the liver ($r=-0.849$, $P<.05$), PRAT ($r=-0.596$, $P<.05$) and circulating PBMCs ($r=-0.961$, $P<.001$), thus indicating that a greater level of p-eIF-2α and therefore an increased ER stress are associated with a lower degree of AMPK phosphorylation. However, no correlation was observed between the degree of AMPK phosphorylation and eIF-2α in SCAT ($r=-0.017$, $P=.475$).

4. Discussion

We show that obese Zucker *fa/fa* rats subjected to a moderate caloric restriction for 2 weeks exhibit a reduced liver weight and hepatic lipid content. This is associated with an increase in AMPK activity together with a reduced expression of ER stress and apoptotic markers, as well as reduced p-eIF-2α/eIF-2α levels. In PRAT, CR increases p-AMPK/AMPK levels, correlating with a reduction of the tissue amount, adipocyte diameter and eIF-2α phosphorylation. Changes elicited in AMPK and eIF-2α by the metabolic status (i.e., obesity or CR) are also detected in circulating PBMCs, suggesting that alterations in these cells might potentially mirror some of the metabolic alterations developed in peripheral tissues.

Several studies performed in different models of obesity such as Zucker *fa/fa* rats [34], lemur male mice [35] or *ob/ob* mice have demonstrated a significant reduction in BW induced by CR, but all of them underwent a severe CR (greater than 40%) or bariatric surgery [26]. Herein, we show that a moderate (20%) and, therefore, a more feasible CR for the patient might reduce body weight, the liver weight and the amount of AT.

AMPK has shown to play a key metabolic role and is able to sense cellular glucose availability as well as its energy status [36]. Interestingly, a reduced activation of AMPK in obesity has been recently described, and it seems to be involved in the development of numerous cardiometabolic alterations [18,19]. In addition, it has been suggested that CR associated with physical exercise as well as the administration of AMPK activators could restore the activity of this protein [18,22]. Accordingly, we have detected a significant reduction of AMPK phosphorylation in the liver, PRAT and PBMCs from *fa/fa* rats as compared with *Lean* C group. Nevertheless, CR significantly improved AMPK phosphorylation in the liver, in PRAT and in PBMCs.

It is also well known that obesity favors the development of ER stress in the liver and in specific adipose depots [26,37], although the exact mechanism is still a matter of debate. Rather than an increase in the rate of misfolded proteins, it is thought that obesity leads to ER stress due to a decrease in the folding capacity and a reduction in the proteasome activity [3]. In the context of our genetic model of obesity, CR successfully reduced hepatic ER stress. We found a significant up-regulation of the UPR markers BiP, eIF-2α, Xbp-1(s), Chop and Caspase3 in the liver of the Zucker *fa/fa* rats, evidencing an overloaded ER and the consequent response leading to a proapoptotic state. Our moderate short-term CR protocol was enough to significantly restore the expression of the aforementioned markers. However, the Bax/Bcl2 ratio was not modified in the liver of the *fa/fa* rats, suggesting that the intrinsic apoptotic pathway is not activated, although caloric restriction produced a 50% reduction in this ratio. Moreover, since the mRNA levels of Bcl2 remain stable among the four experimental groups, the reduction of the apoptotic signal in *fa/fa* CR rats is apparently due to a decrease in the apoptotic signal rather than an increase in prosurvival pathways. A similar reduction of ER stress mediated by CR has also been described in models of diet-induced obesity [38] or diabetes [39]. In the same line, Tsutsumi et al. observed a normalization of p-eIF-2α levels in *ob/ob* obese mice after a 50% CR [26]. However, our results indicate for the first time that it is not necessary to subject the animals to an aggressive CR to obtain a reduction of ER stress since similar effects were achieved with a moderate, much more physiological CR. Interestingly, in our model, PRAT from obese rats was less severely affected by ER stress since no up-regulation of the extrinsic apoptotic branch (Chop, caspase 3) was observed, and only an increase in the mRNA levels of the chaperones Edem and Pdia-4 was detected, with a limited effect of CR to moderate the response. Nevertheless, an increased ratio p-eIF-2α/eIF-2α was detected in PRAT from Zucker *fa/fa* rats, and it was significantly reduced by CR. Studies in humans have described the presence of ER stress in the adipose tissue of obese patients [40,41] and its reduction 1 year after gastric bypass surgery [42]. Interestingly, in our model, we have observed a clear association between ER stress (p-eIF-2α) and p-AMPK in the liver and PRAT, where higher AMPK phosphorylation was associated with lower ER stress. Those results support other studies performed in other peripheral tissues like the kidneys or the vasculature showing a link between ER stress and AMPK activity [23–25]. However, further studies would be required to better clarify how ER stress might be modulated by AMPK activity and/or *vice versa*.

According to our results, the preexisting metabolic state seems to be critical to define the impact of CR in ER stress. In our model, CR triggered the UPR in *Lean* animals mainly in the PRAT, characterized by an up-regulation of eIF-2α and Xbp-1(s) expression. This suggests that CR promotes the activation of the reparatory branches of the UPR, which could be an indicator of a moderate ER stress. Apparently, a similar situation could be taking place in the liver, although further experiments would be required to elucidate this point. In this direction, a study performed by Chan et al. demonstrated that early-life exposure to undernutrition induced ER stress [43]. Similarly, several studies have evidenced that low-protein diet might also favor ER stress [44,45]. In fact, CR in *Lean* humans promoted increased expression of chaperones such as Hsp70 or Grp78 as well as autophagic mediators [46].

Intriguingly, CR did not reduce adipocyte diameter or improve AMPK phosphorylation in SCAT. These results support the higher susceptibility to CR exerted by the liver and PRAT in comparison with SCAT and are in accordance with the study performed by Narita et al. that evidenced a higher response of retroperitoneal adipocytes compared to subcutaneous adipocytes to the effect of CR [47] and with the fact that visceral AT exerts a higher lipolytic activity than SCAT [48]. In addition and since ER stress was significantly reduced by CR in SCAT, those results suggest that alterations associated with ER stress might be reversed earlier than those related to AMPK activation and that ER stress might be a more sensitive marker of metabolic changes than AMPK activity. Therefore, we might speculate that we would probably observe the same effect in p-AMPK/AMPK ratio in SCAT if CR was maintained for a longer period.

In the circulating PBMCs obtained from blood samples, the protein levels of p-eIF-2α mimic the pattern observed in liver and PRAT, characterized by (1) the activation of eiF-2α in the *fa/fa* Zucker rats, (2) the amelioration after CR in obese animals and (3) the activation of eiF-2α by CR in *Lean* animals in the adipose depots. In a similar manner, a recent study by López-Domenech et al. described the use of lymphocytes to assess the effect of 24 weeks of dietary treatment on UPR pathways during ER stress, redox status and mitochondrial function in obese patients [49].

A limitation of this study is that, because of the limited amount of PBMCs that we could isolate from rats, we did not analyze UPR response in PBMCs and we could not establish a functional relationship between CR and ER stress in PBMCs. Therefore, and despite several studies that have suggested that alterations detected in PBMCs might mirror the ones observed in other peripheral tissues

[20,49], further experiments would be required to elucidate whether PBMCs could be used for the screening of early metabolic disorders.

In conclusion, this study demonstrates that CR in obesity reduces ER stress and improves AMPK activation, contributing to ameliorating metabolic disorders associated with obesity. Since those effects are also observed in PBMCs, they could constitute a potential interesting tool to assess both ER stress development and AMPK alterations during the onset of obesity. Consequently, the finding of circulating cells that might reflect the physiological state of the obese individuals like PBMCs might provide new insights into an early detection of metabolic alterations and the prevention of several comorbidities derived from obesity.

Supplementary data to this article can be found online at https://doi.org/10.1016/j.jnutbio.2020.108342.

Acknowledgments

We wish to acknowledge J.M. Garrido, J. Bravo and I. Bordallo for skillful animal care during the experiment and Dolores Morales for her help with the confocal microscope. This work was supported by grants from Ministerio de Economía y Competitividad (BFU2011-25303), Grupos UCM (GR-921641), Fundación Universitaria San Pablo-CEU, Fundación Mutua Madrileña, Fundación de Estudios Metabólicos and SESCAMET. V.-M.E. is a recipient of a Comunidad de Madrid fellowship, M.-L.F.J. and G.-P.C.F. are recipients of a Ministerio de Educación, Cultura y Deporte fellowships and G.-.B.R. of a fellowship of Fundación Universitaria CEU San Pablo.

Declaration of competing interest

The authors declare no competing financial interests.

References

[1] Lin Chun TH, Kang L. Adipose extracellular matrix remodelling in obesity and insulin resistance. Biochem Pharmacol 2016;119:8–16.
[2] Hotamisligil GS. Inflammation and metabolic disorders. Nature 2006;444:860–7.
[3] Pagliassotti MJ, Kim PY, Estrada AL, Stewart CM, Gentile CL. Endoplasmic reticulum stress in obesity and obesity-related disorders: an expanded view. Metabolism: clinical and experimental 2016;65:1238–46.
[4] Gregor MF, Hotamisligil GS. Thematic review series: adipocyte biology. Adipocyte stress: the endoplasmic reticulum and metabolic disease. J Lipid Res 2007;48:1905–14.
[5] Kassan M, Galan M, Partyka M, Saifudeen Z, Henrion D, Trebak M, et al. Endoplasmic reticulum stress is involved in cardiac damage and vascular endothelial dysfunction in hypertensive mice. Arterioscler Thromb Vasc Biol 2012;32:1652–61.
[6] Young CN. Endoplasmic reticulum stress in the pathogenesis of hypertension. Exp Physiol 2017;102:869–84.
[7] Lionetti L, Mollica MP, Lombardi A, Cavaliere G, Gifuni G, Barletta A. From chronic overnutrition to insulin resistance: the role of fat-storing capacity and inflammation. Nutr Metab Cardiovasc Dis 2009;19:146–52.
[8] Mollica MP, Lionetti L, Putti R, Cavaliere G, Gaita M, Barletta A. From chronic overfeeding to hepatic injury: role of endoplasmic reticulum stress and inflammation. Nutr Metab Cardiovasc Dis 2011;21:222–30.
[9] Lee AS. The ER chaperone and signaling regulator GRP78/BiP as a monitor of endoplasmic reticulum stress. Methods 2005;35:373–81.
[10] Kaufman RJ. Orchestrating the unfolded protein response in health and disease. J Clin Invest 2002;110:1389–98.
[11] Rutkowski DT, Kaufman RJ. A trip to the ER: coping with stress. Trends Cell Biol 2004;14:20–8.
[12] Calfon M, Zeng H, Urano F, Till JH, Hubbard SR, Harding HP, et al. IRE1 couples endoplasmic reticulum load to secretory capacity by processing the XBP-1 mRNA. Nature 2002;415:92–6.
[13] Shen X, Ellis RE, Lee K, Liu CY, Yang K, Solomon A, et al. Complementary signaling pathways regulate the unfolded protein response and are required for *C. elegans* development Cell 2001;107:893–903.
[14] Yoshida H, Matsui T, Hosokawa N, Kaufman RJ, Nagata K. Mori K. a time-dependent phase shift in the mammalian unfolded protein response. Dev Cell 2003;4:265–71.
[15] Yoshida H, Matsui T, Yamamoto A, Okada T, Mori K. XBP1 mRNA is induced by ATF6 and spliced by IRE1 in response to ER stress to produce a highly active transcription factor. Cell 2001;107:881–91.
[16] Yamaguchi H. Wang HG. CHOP is involved in endoplasmic reticulum stress-induced apoptosis by enhancing DR5 expression in human carcinoma cells. J Biol Chem 2004;279:45495–502.
[17] Hardie DG. AMP-activated/SNF1 protein kinases: conserved guardians of cellular energy. Nat Rev Mol Cell Biol 2007;8:774–85.
[18] Ruderman NB, Carling D, Prentki M, Cacicedo JM. AMPK, insulin resistance and the metabolic syndrome. J Clin Invest 2013;123:2764–72.
[19] Gauthier MS, O'Brien EL, Bigornia S, Mott M, Cacicedo JM, Xu XJ, et al. Decreased AMP-activated protein kinase activity is associated with increased inflammation in visceral adipose tissue and with whole-body insulin resistance in morbidly obese humans. Biochem Biophys Res Commun 2011;404:382–7.
[20] García-Prieto CF, Gil-Ortega M, Vega-Martín E, Ramiro-Cortijo D, Martín-Ramos M, Bordiú E, et al. Beneficial effect of bariatric surgery on abnormal MMP-9 and AMPK activities: potential markers of obesity-related CV risk Frontiers in physiology; 2019.
[21] Pires RC, Souza EE, Vanzela EC, Ribeiro RA, Silva-Santos JC, Carneiro EM, et al. Short-term calorie restriction improves glucose homeostasis in old rats: involvement of AMPK. Appl Physiol Nutr Metab 2014;39:895–901.
[22] Garcia-Prieto CF, Pulido-Olmo H, Ruiz-Hurtado G, Gil-Ortega M, Aranguez I, Rubio MA, et al. Mild caloric restriction reduces blood pressure and activates endothelial AMPK-PI3K-Akt-eNOS pathway in obese Zucker rats. Vascul Pharmacol 2015;65-66:3–12.
[23] Dong Y, Zhang M, Liang B, Xie Z, Zhao Z, Asfa S, et al. Reduction of AMP-activated protein kinase alpha2 increases endoplasmic reticulum stress and atherosclerosis in vivo. Circulation 2010;121:792–803.
[24] Kim H, Moon SY, Kim JS, Baek CH, Kim M, Min JY, et al. Activation of AMP-activated protein kinase inhibits ER stress and renal fibrosis. Am J Physiol Renal Physiol 2015;308:F226–36.
[25] Li J, Wang Y, Wang Y, Wen X, Ma XN, Chen W, et al. Pharmacological activation of AMPK prevents Drp1-mediated mitochondrial fission and alleviates endoplasmic reticulum stress-associated endothelial dysfunction. J Mol Cell Cardiol 2015;86:62–74.
[26] Tsutsumi A, Motoshima H, Kondo T, Kawasaki S, Matsumura T, Hanatani S, et al. Caloric restriction decreases ER stress in liver and adipose tissue in Ob/Ob mice. Biochem Biophys Res Commun 2011;404:339–44.
[27] Briet F, Twomey C, Jeejeebhoy KN. Relationship between metabolism and peripheral blood mononuclear cell mitochondrial complex I activity before and after a short-term refeeding in weight-losing cancer patients. Clin Nutr 2003;22:247–53.
[28] Cortez E, Neves FA, Bernardo AF, Stumbo AC, Carvalho L, Garcia-Souza E, et al. Lymphocytes mitochondrial physiology as biomarker of energy metabolism during fasted and fed conditions. ScientificWorldJournal 2012;2012:629326.
[29] Kilkenny C, Browne W, Cuthill IC, Emerson M, Altman DG, Group NCRRGW. Animal research: reporting in vivo experiments: the ARRIVE guidelines. Br J Pharmacol 2010;160:1577–9.
[30] McGrath JC, Drummond GB, McLachlan EM, Kilkenny C, Wainwright CL. Guidelines for reporting experiments involving animals: the ARRIVE guidelines. Br J Pharmacol 2010;160:1573–6.
[31] Herrera E, Ayanz A. Calculation of lipolysis and esterification from glycerol metabolism in rat adipose tissue. J Lipid Res 1972;13:802–9.
[32] Bradford MM. A rapid and sensitive method for the quantitation of microgram quantities of protein utilizing the principle of protein-dye binding. Anal Biochem 1976;72:248–54.
[33] Somoza B, Guzman R, Cano V, Merino B, Ramos P, Diez-Fernandez C, et al. Induction of cardiac uncoupling protein-2 expression and adenosine 5′-monophosphate-activated protein kinase phosphorylation during early states of diet-induced obesity in mice. Endocrinology 2007;148:924–31.
[34] Bankoglu EE, Seyfried F, Rotzinger L, Nordbeck A, Corteville C, Jurowich C, et al. Impact of weight loss induced by gastric bypass or caloric restriction on oxidative stress and genomic damage in obese Zucker rats. Free Radic Biol Med 2016;94:208–17.
[35] Villain N, Picq JL, Aujard F, Pifferi F. Body mass loss correlates with cognitive performance in primates under acute caloric restriction conditions. Behav Brain Res 2016;305:157–63.
[36] Lin SC, Hardie DG. AMPK: Sensing glucose as well as cellular energy status. Cell Metab 2018;27:299–313.
[37] Zhou H. Liu R. ER stress and hepatic lipid metabolism. Front Genet 2014;5:112.
[38] Ding S, Jiang J, Zhang G, Bu Y, Zhang G, Zhao X. Resveratrol and caloric restriction prevent hepatic steatosis by regulating SIRT1-autophagy pathway and alleviating endoplasmic reticulum stress in high-fat diet-fed rats. PloS one 2017;12:e0183541.
[39] Kanda Y, Hashiramoto M, Shimoda M, Hamamoto S, Tawaramoto K, Kimura T, et al. Dietary restriction preserves the mass and function of pancreatic beta cells via cell kinetic regulation and suppression of oxidative/ER stress in diabetic mice. J Nutr Biochem 2015;26:219–26.
[40] Boden G, Duan X, Homko C, Molina EJ, Song W, Perez O, et al. Increase in endoplasmic reticulum stress-related proteins and genes in adipose tissue of obese, insulin-resistant individuals. Diabetes 2008;57:2438–44.
[41] Sharma NK, Das SK, Mondal AK, Hackney OG, Chu WS, Kern PA, et al. Endoplasmic reticulum stress markers are associated with obesity in nondiabetic subjects. J Clin Endocrinol Metab 2008;93:4532–41.
[42] Gregor MF, Yang L, Fabbrini E, Mohammed BS, Eagon JC, Hotamisligil GS, et al. Endoplasmic reticulum stress is reduced in tissues of obese subjects after weight loss. Diabetes 2009;58:693–700.
[43] Chan KA, Bernal AB, Vickers MH, Gohir W, Petrik JJ, Sloboda DM. Early life exposure to undernutrition induces ER stress, apoptosis, and reduced vascularization in ovaries of adult rat offspring. Biol Reprod 2015;92:110.

[44] Yokota S, Ando M, Aoyama S, Nakamura K, Shibata S. Leucine restores murine hepatic triglyceride accumulation induced by a low-protein diet by suppressing autophagy and excessive endoplasmic reticulum stress. Amino Acids 2016;48:1013–21.
[45] Batista TM, da Silva PM, Amaral AG, Ribeiro RA, Boschero AC, Carneiro EM. Taurine supplementation restores insulin secretion and reduces ER stress markers in protein-malnourished mice. Adv Exp Med Biol 2013;776:129–39.
[46] Yang L, Licastro D, Cava E, Veronese N, Spelta F, Rizza W, et al. Long-term calorie restriction enhances cellular quality-control processes in human skeletal muscle. Cell Rep 2016;14:422–8.
[47] Narita T, Kobayashi M, Itakura K, Itagawa R, Kabaya R, Sudo Y, et al. Differential response to caloric restriction of retroperitoneal, epididymal, and subcutaneous adipose tissue depots in rats. Exp Gerontol 2018;104:127–37.
[48] Engfeldt P, Arner P. Lipolysis in human adipocytes, effects of cell size, age and of regional differences. Horm Metab Res Suppl 1988;19:26–9.
[49] Lopez-Domenech S, Abad-Jimenez Z, Iannantuoni F, de Maranon AM, Rovira-Llopis S, Morillas C, et al. Moderate weight loss attenuates chronic endoplasmic reticulum stress and mitochondrial dysfunction in human obesity. Mol Metab 2019;19:24–33.